Saudi Pharmaceutical Journal 32 (2024) 102099

HOSTED BY

Contents lists available at ScienceDirect

Saudi Pharmaceutical Journal

journal homepage: www.sciencedirect.com

Original article

Formulation, development and evaluation of hyaluronic acid-conjugated liposomal nanoparticles loaded with regorafenib and curcumin and their in vitro evaluation on colorectal cancer cell lines

Sewar G. Shnaikat [a], Ashok K. Shakya [a,*], Sanaa K. Bardaweel [b]

[a] Faculty of Pharmacy, Al-Ahliyya Amman University, Amman, Jordan
[b] School of Pharmacy, The University of Jordan, Amman, Jordan

ARTICLE INFO

Keywords:
Liposome
Hyaluronic acid
Regorafenib
Curcumin
CD44
Targeted drug delivery
Colorectal cancer

ABSTRACT

Colorectal cancer is one of the major causes of global cancer, with chemotherapy and radiation therapy being effective but limited due to low specificity. Regorafenib, a multikinase inhibitor, provides hope to patients with metastatic colorectal cancer and was approved by the FDA in 2012. However, due to resistance issues and adverse events, its efficacy is compromised, necessitating further refinement. Meanwhile, curcumin, a compound of turmeric, exhibits anticancer effects through antioxidant and anti-inflammatory actions, induction of the apoptosis, arrest of cell cycle, inhibition of angiogenesis, and modulation of signaling pathways. Unfortunately, its clinical utility is limited by its poor bioavailability, pointing towards innovative drug delivery strategies for enhanced efficacy in colorectal cancer treatment.

Hyaluronic acid (HA)-decorated liposomes (LIPO) have been developed to target colorectal cells through an overexpressed CD44 receptor, increasing antitumor and antimetastasis efficacy. This study investigates the possibility of loading curcumin (CUR) or regorafenib (REGO) into a liposomal formulation for passive and HA-actively targeted treatment, evaluating its critical quality attributes (CQA) (size, zeta potential, polydispersity index) and cytotoxic activity in the HT29 colorectal cancer cell line. The average particle size of the plain liposomes and those decorated with HA was 144.00 ± 0.78 nm and 140.77 ± 1.64 nm, respectively. In contrast, curcumin-loaded plain liposomes and HA-decorated liposomes had 140 ± 2.46 nm and 164.53 ± 15.13 nm, respectively. The prepared liposomes had a spherical shape with a narrow size distribution and an acceptable zeta potential of less than −30 mV. The encapsulation efficiency was 99.2 % ± 0.3 and 99.9 ± 0.2 % for HA-decorated and bare regorafenib loaded. The % EE was 98.9 ± 0.2 % and 97.5 ± 0.2 % for bare liposomal nanoparticles loaded with curcumin and coated with curcumin. The IC_{50} of free REGO, CUR, REGO-LIPO, CUR-LIPO, REGO-LIPO-HA and CUR-LIPO-HA were 20.17 ± 0.78, 64.4 ± 0.33, 224.8 ± 0.06, 49.66 ± 0.22, 73.66 ± 0.6, and 27.86 ± 0.49 μM, respectively. The MTT assay in HT29 cells showed significant cytotoxic activity of the HA-decorated liposomal formulation compared to the base uncoated formulation, indicating that hyaluronic acid-targeted liposomes loaded with regorafenib or curcumin could be a promising targeted formulation against colorectal cancer cells.

1. Introduction

As the third leading cause of cancer-related death globally, colorectal cancer (CRC) accounts for more than 1.85 million new cases and 850,000 deaths a year with a cumulative incidence risk of 2.27 % between 0 and 74 years of age (Gunter et al., 2019; Mattiuzzi et al., 2019; Xie et al., 2020). 20 % of new colorectal cell diagnoses have metastatic cancer at presentation, and another 25 % of patients with localized disease might develop metastases subsequently (Biller & Schrag, 2021). Recent advances in disease understanding have ultimately resulted in many therapeutic approaches, including surgical intervention, radiation and chemotherapy, as well as targeted therapy and multitherapy (Kumar et al., 2021; Sang et al., 2021).

The toxic effects of chemotherapy and radiation therapy on healthy tissues and drug resistance significantly affect the quality of life and cancer-specific objectives, in addition to their adverse effects on

* Corresponding author at: Pharmacological and Diagnostic Research Center, Faculty of Pharmacy, Al-Ahliyya Amman University, Amman, Jordan.
E-mail address: ak_shakya@ammanu.edu.jo (A.K. Shakya).

https://doi.org/10.1016/j.jsps.2024.102099
Received 25 February 2024; Accepted 12 May 2024
Available online 18 May 2024

patients, including pain, nausea, diarrhea, hair loss, and others. This signifies the need for treatment improvement, including new drug delivery methods to overcome these limitations (Sang et al., 2021; Scaria et al., 2020).

For example, Regorafenib (REGO) (BAY 73–4506, Stivarga®) is a small molecule multikinase inhibitor that was approved by the FDA in 2012 for patients with metastatic colorectal cancer (Fig. 1) (Crona et al., 2013; Ettrich & Seufferlein, 2018; Strumberg & Schultheis, 2012). It is an inhibitor of tyrosine kinase of angiogenic, stromal and oncogenic receptor tyrosine kinase inhibitor (Wilhelm et al., 2011). REGO has shown promising results in patients with advanced, unresectable, or metastatic GISTs and has been shown to improve survival after standard therapies have failed. The problem at hand is that a large proportion of patients encountered treatment-related adverse events (AEs), many of which were considered either moderate or mild in severity, dermatological toxicities and elevated liver enzymes being the most prevalent AEs (Dhillon, 2018). Furthermore, in some cases of colorectal cancer, the principle of regorafenib resistance is widely undefined (Mirone et al., 2016).

Another example includes curcumin (CUR), which is an organic substance derived from the perennial herb *Curcuma longa* (turmeric), also known as diferuloylmethane (Hewlings & Kalman, 2017; Mahmoudi et al., 2021; Sharifi-Rad et al., 2020). It is a natural polyphenol derived from the root of Curcuma longa Linn, despite its hydrophobic nature and alkaline pH, demonstrating anticancer potential (Bardania et al., 2023; Fazli et al., 2022).

Curcuminoids (CCM) are biologically active polyphenolic compounds isolated from turmeric that include curcumin (CUR), demethoxycurcumin (DMC), and bisdemethoxycurcumin (BDMC) (Amekyeh et al., 2022). Curcumin has attracted extensive research as an anticancer drug due to its ability to control key cellular signaling pathways such as signal transducer and activation transcription (STAT) proteins, activated protein-1 (AP-1), epidermal growth response-1 (Egr-1) and p53, 5-lipoxygenases, cyclooxygenase-2, urinary plasminogen activator, mitogen-activated protein kinases (MAPK), all of which are involved in cancer development, differentiation, and survival (Bardania et al., 2023; Wong et al., 2019). Despite this, the clinical application of CUR is severely limited due to its hydrophobic nature, poor oral absorption, low bioavailability, chemical instability, photodegradation, and rapid metabolism (Tefas et al., 2017; Wong et al., 2019).

All the mentioned drawbacks can be solved by different drug delivery methods. Liposomes were among the most successful nanocarrier candidates in targeted delivery of oncological treatment, improving the safety profile and therapeutic effects of the trapped drug (Sang et al., 2021; Tefas et al., 2017).

Liposomal nanoparticles offer enhanced biocompatibility, fewer side effects, better antitumor activity, and longer drug accumulation compared to free drugs (Chen et al., 2022; Sang et al., 2021; Tefas et al., 2017). They can also be used for the co-administration of multiple medications, as the standard single-drug chemotherapeutic regimen is not ideal (Olusanya et al., 2018; S. Wang et al., 2023). Liposomes have several advantages, including cell-like membrane structure, nanoscale features, high compatibility, low immunogenicity, protection of the drug or its active group, prolongation of the drug half-life, decreased toxicity, and improved effectiveness, making them a valuable drug delivery technique in pharmaceutical research (Guimarães et al., 2021; Li et al., 2019; Tefas et al., 2017).

Recent studies in the field of cancer treatment focus on active targeting through conjugation of tumor-specific ligands to the external layer of liposomal phospholipid bilayers (Ravar et al., 2016). To improve liposomal delivery systems for colorectal cancer, structural and surface modifications based on conventional lipid molecules have been made to produce unique biological effects. However, the Mononuclear Phagocyte System (MPS) rapidly consumes conventional liposomes, causing a rapid drop in drug concentration and accumulation in organs, reducing drug delivery, and potentially harming stored organs. Surface modifications to produce long-circulating liposomes (LCL) and actively targeted liposomes can help overcome this problem (Li et al., 2019; Ravar et al., 2016).

Long-circulating liposomes (LCLs) are coated with inert polymeric molecules, such as oligosaccharides, polysaccharides, glycoproteins, and synthetic polymers. One such hydrophilic polysaccharide is hyaluronic acid (HA), a naturally occurring linear hydrophilic polysaccharide (Liu et al., 2011; Ravar et al., 2016; Tiantian et al., 2014). HA is a promising candidate for targeted nanocarrier delivery due to its biocompatibility, biodegradability, nontoxic and non-immunogenic

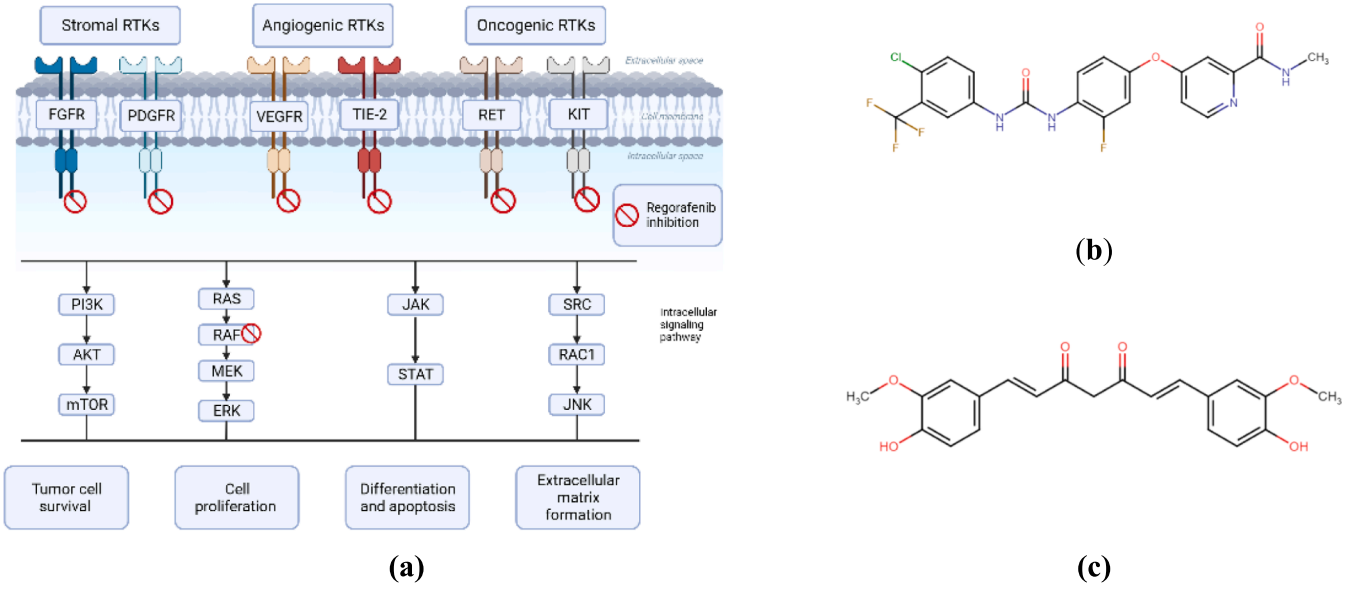

Fig. 1. Structure and mechanism of action. (a) The mechanisms of regorafenib anti-tumor activity. Regorafenib blocks multiple active pathways involved in angiogenesis, tumor cell survival, cell proliferation, differentiation, apoptosis, and extracellular matrix formation. This offers potential explanations for its anti-tumor effectiveness in colorectal cancer. Created with BioRender.com. (b) Chemical structure of regorafenib. Created with chem-space.com. (c) Chemical structure of curcumin. Created with chem-space.com..

nature, numerous functional groups for modification, and diverse sources (Pandolfi et al., 2019; Ravar et al., 2016; Rippe et al., 2019). The main cell surface receptor is the cluster of Differentiation 44 (CD44), an extracellular protein on the cell's outer membrane. This receptor is overexpressed in cancerous tissue, including melanoma, lymphoma, colorectal, breast, and lung cancer (Eliaz & Szoka, 2001; Ravar et al., 2016; Yang et al., 2013). HA is a suitable substitute for PEG, binding to high affinity tumor recognition sites (CD44) receptors, facilitating endocytosis into cells, and facilitating drug circulation (Fig. 2) (Misra et al., 2015; Qhattal et al., 2014; Ravar et al., 2016).

HA-decorated liposomes offer a promising strategy for targeted drug delivery in colorectal cancer therapy. By conjugating HA, a ligand for the overexpressed CD44 receptor in many cancer cells, these liposomes can specifically target colorectal tumor cells (Eliaz & Szoka, 2001; Ravar et al., 2016). This active targeting approach enhances the selectivity of drug delivery and minimizes off-target effects, thereby reducing toxicity to healthy tissues. Furthermore, the HA coating provides a hydrophilic cover for liposomes, preventing opsonin adsorption and increasing circulation time, leading to prolonged drug exposure in the tumor microenvironment (Ravar et al., 2016).

The therapeutic efficacy of encapsulated drugs such as regorafenib and curcumin can be optimized by utilizing HA-decorated liposomes. These liposomes not only enhance the biocompatibility and safety profile of trapped drugs but also allow the co-delivery of multiple medications, addressing the limitations of single-drug chemotherapeutic regimens (Tefas et al., 2017).

The purpose of this study was to create bare and HA-decorated liposomes as nanoparticles for passive and active targeted delivery of either regorafenib or curcumin and to evaluate their anticancer effects on the proliferation of CD44-expressing HT29 colorectal cancer cells (Elliott et al., 2014).

2. Materials and methods

2.1. Materials

Dioleoyl phosphatidylethanolamine (DOPE), dipalmitoyl phosphatidylcholine (DPPC), dipalmitoyl phosphatidylglycerol (DPPG), cholesterol and curcumin (CAS no. 458-37-7) were purchased from Sigma Aldrich (USA). The sodium salt of hyaluronic acid, 1-ethyl-3-(3-dimethyl aminopropyl)-carbodiimide (EDC), and N-hydroxysuccinimide (NHS) were purchased from (Sigma Aldrich /product of Japan). The passage of human HT29 colon cancer cells was brought from ECACC. Regorafenib (BAY 73-4506, CAS Number: 755037-03-7) was purchased from the Tokyo Chemical Industry, Tokyo, Japan. Dialysis bag Spectra/Por® 7 (MWCO 10,000, 12 mm), dimethylsulfoxide (DMSO) and Dulbecco's modified medium–high glucose (DMEM-high glucose), formic acid, orthophosphoric acid (85 %, AR), phosphate buffered saline tablets, Promega kit for the MTT assay, and chloroform were also purchased from Sigma-Aldrich (USA). Fetal bovine serum (FBS), L-glutamine, trypsin, and penicillin/streptomycin were purchased from Euro-clone (Italy). All HPLC-grade solvents were purchased from Sigma-Aldrich, USA.

2.2. Methods

2.2.1. Preparation of blank, REGO, and CUR loaded liposomes

To formulate an appropriate liposomal formulation with respect to lipid composition and HA coating for active targeting of CUR and REGO, keeping in mind that both are lipophilic compounds that will be loaded into the phospholipid bilayer of the liposome, a few studies on the liposomal formulation were demonstrated as references in the following (Table 1).

Based on the information in (Table 1), a suitable combination of (DPPC, DPPG, DOPE, and cholesterol) was chosen for the encapsulation of CUR and REGO. Dipalmitoylphosphoglycerol (DPPG) was added to further stabilize the liposomal formulation and achieve good colloidal stability because the negative charge on the outer surface of the vesicle

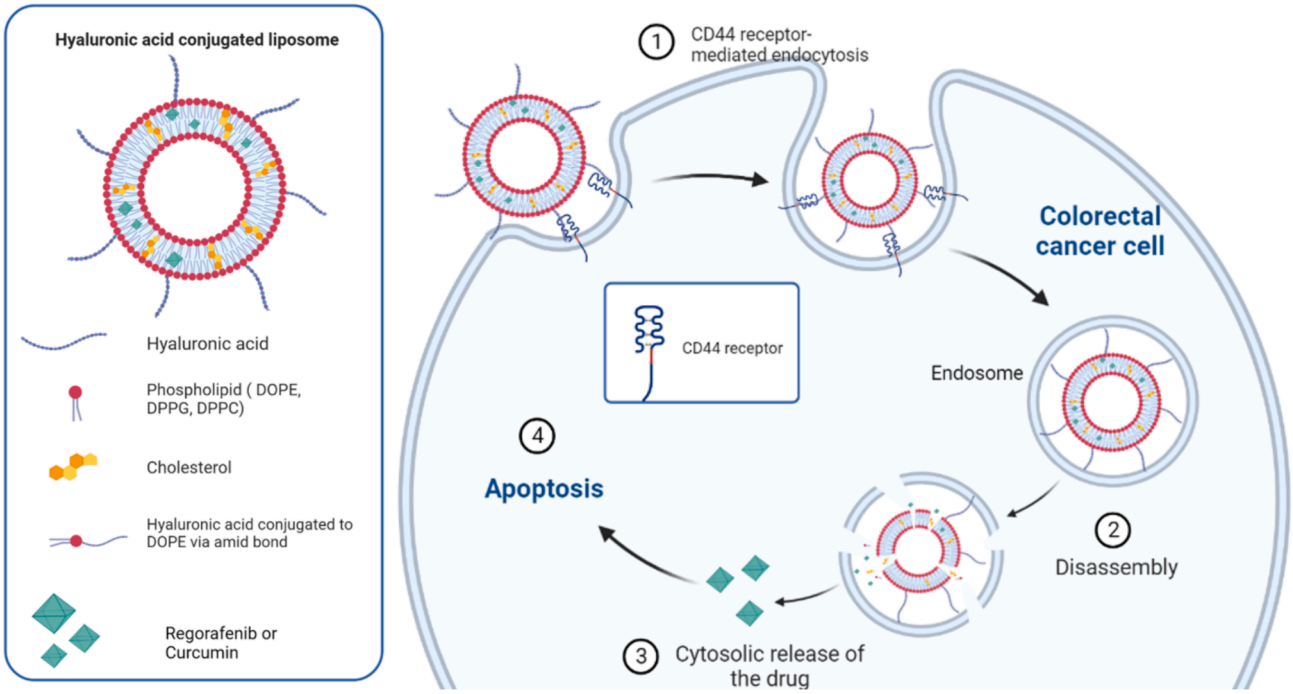

Fig. 2. The basic structure and schematic illustration of regorafenib or curcumin-loaded HA-decorated liposomes. The CD44 receptor, which is overexpressed in colorectal tumor cells, is specifically liganded by the HA molecule. Cellular uptake of liposomes was enhanced by CD44-mediated endocytosis. Created with BioRender.com.

Table 1
A review of different liposomal formulations available in the literature.

Drugs Encapsulated	Liposomal NP Type	Method Of Preparation	Critical Quality Attributes (CQAs)	Cancer Cell Line/ (IC_{50} Of Nps)	In Vitro Release Test	Study Authors (Reference)
CUR	egg-phosphatidylcholine (EPC) liposomes.	thin-film hydration method	size: 108.0 ± 8.9 nm ZP: EE: 85 %	(HCT116, HCT15, Colo205 and DLD-1) IC_{50}: < 6 μM vs 4.5–47.3 μM	Curcumin release at 96hrs 14.11 % ±2.56	(Pandelidou et al., 2011)
CUR + CaCO3	PH-sensitive NPs Soybean lecithin (SPC), DSPE-PEG2000, CHEMS	W/O emulsion-mediated film dispersion method	size: 155.3 ± 3.8 nm, ZP: −14.2 ± 0.3 mV EE: 77.67 ± 1.82 %	HCT-116 The (IC50) of free CUR, CUR-LIPO and lipid/CaCO3/CUR (LCC) were 9.413, 7.166, and 5.067 μM, respectively.	fast release of curcumin at pH 5.5	(Chen et al., 2019)
CUR And Doxorubicin (DOX)	Long-circulating liposomes (LCL) DPPC PEG-2000-DSPE sodium salt Cholesterol	Thin-film-hydration method	size: 182.00 ± 1.22 nm PI: 0.07 ± 0.01 Zp: −42.30 ± 0.20 mv % EE of CUR: 87.48 ± 1.86, DOX: 38.41 ± 0.13	C26 murine cells IC_{50}:CUR: 4.50 ± 0.06 mM DOX: 0.02 ± 0.00 mM	——	(Sesarman et al., 2018)
CUR			size: 180.10 ± 3.06 nm PI: 0.08 ± 0.01 ZP: −38.10 ± 1.76mv % EE: 66.78 ± 0.58	C26 murine cells IC_{50}: 4.75 ± 0.04 mM		
5-Fluorouracil (5-FU)	HA conjugated. DOPE, DOTAP, and des PEG2000	Thin film hydration method	Bare liposome % EE 2 ± 4.54 % Size 112 ± 28 PDI 0.15 HA-LIPO % EE 91 % size 144 ± 77 nm PDI 0.2,	HT29 IC50 at 72 h of free 5FU was 35 μg/mL, for 5FUlipo was 8 μg/mL and for 5FUlipoHA was 4 μg/mL	Drug release −HA-liposomes: 40 % after 10 hr	(Mansoori et al., 2020)
honokiol (HNK)	HA conjugated. PC, DOPE, DOTAP, cholesterol	Thin film hydration method	HA-Lip-HNK complex size162.6 ± 3.8 nm PDI 0.26 ± 0.02. % EE: 9.3 %-92.5.	4T1murine The IC50 values of free HNK, Lip-HNK and HA-Lip-HNK were calculated to be 2.41 ± 0.12, 3.77 ± 0.17 and 6.97 ± 0.27 μg/mL, respectively	cumulative release was 62.1 %	(J. Wang et al., 2020)
Paclitaxel	HA conjugated. DPPC DOTAP cholesterol	Thin film hydration method	% EE:93.4 ± 2.9 size of 106.4 ± 3.2 nm zetapotential of −9.7 ± 0.8Mv PDI 0.22 ± 0.07	4T1murine and T47D cells HA-Lipo / PTX showed a lower IC50 than that of Lipo/PTX($p < 0.05$) or free PTX solution (p0.05) in both cell lines	Release of 95 % in 40 h.	(Ravar et al., 2016)

Table 1. Abbreviations: (CUR) curcumin; (EE) encapsulation efficiency; (IC_{50}) half maximum inhibitory concentration; (N/D) not determined; (N/I) not indicated; (NP) nanoparticle; (PEG) polyethylene glycol; (PBS) phosphate buffered saline; (ZP) zeta potential, (DPPC) 1,2-Dipalmitoyl-*sn*-glycero-3-phosphocholine; (PEG-2000-DSPE sodium salt) polyethylene glycol- 2000–1,2-distearoyl-*sn*-glycero-3 sodium salt; (CHEMS) cholesteryl hemi succinate; (HNK) honokiol; (5-FU) 5-flourouracil; (HA) hyaluronic acid; (DOTAP)1,2-dioleoyl-3-trimethylammonium propane.

causes vesicle-vesicle repulsion; therefore, the use of negatively charged DPPG in our liposomal preparation might be beneficial. Incorporation of a charge-inducing agent into the liposomal preparation increases the electrostatic repulsion energy, preventing the aggregation and fusion of vesicles, and thus increasing the shelf life (Ho et al., 2023).

The thin film hydration method was used to prepare all liposomes according to the methods available in the literature with slight modifications (Lombardo & Kiselev, 2022; Zhang, 2017).

2.2.1.1. Preparation of the blank liposome. In a round bottom flask, 3 ml of chloroform was used to dissolve a mixture of DOPE (3 mg) DPPC (3 mg) DPPG (3 mg) and cholesterol (3 mg). The chloroform was then evaporated to dryness under vacuum using a rotary evaporator at a temperature of 40 °C, starting with a pressure of 500 mbar reduced by 50 mbar every 15 min until it reached 100 mbar, to obtain a thin lipid film.

The evaporation temperature of 40 °C is selected to ensure gradual evaporation of chloroform below its boiling point (61 °C at standard pressure), preventing lipid degradation and phase transitions. This temperature promotes thin, uniform film formation, facilitating subsequent liposome preparation steps and maintaining lipid stability by staying below their transition temperatures (John et al., 2024; Leonenko et al., 2004; Pan et al., 2012).

Subsequently, the thin film was flushed with nitrogen and kept in the freezer (−20 °C) overnight to stabilize the lipids. The lipid film was hydrated the following day with 3 ml of phosphate buffer saline (PBS), pH 7.4, and the bath sonicator for 3 h with occasional vortexing. This forms drug-loaded heterogeneous multilaminar vesicles (MLV) liposomal vesicles. The liposomes formed were refrigerated (Lombardo & Kiselev, 2022; Zhang, 2017).

Size reduction was carried out by sonication and/or extrusion (Ong et al., 2016). In different batches of liposomes prepared as previously described, with slight modifications to obtain unilaminar vesicles (ULV). To obtain a normal distribution of the liposomal vesicles with an acceptable size of ~200 nm, the probe sonication with a 25 % amplitude (Bandelin, Germany, Model Number-UW100, Probe TS103) was used, which provides large unilaminar vesicles (LUVs) with the desired size. The second is the extrusion of MLV using the Avanti Mini-Extruder set with different polycarbonate membranes (from 400 nm down to 100 nm) (Szoka and Papahadjopoulos, 1980; Zhu et al., 2013; (Andra et al., 2022).

2.2.1.2. Preparation of regorafenib liposomes. The regorafenib loaded liposomes were prepared using the method described in Section 2.2.1.1. All desired contents were dissolved in 3 ml of chloroform, including accurately weighed regorafenib (1 mg).

2.2.1.3. Preparation of curcumin liposomes. It was prepared using the method described in Section 2.2.1.2 using 1 mg of curcumin instead of regorafenib.

2.2.2. Hyaluronic acid-coated liposomes

The liposome surface (especially the functional groups) was modified using HA to form an amide bond as described in the literature with minor modifications (Mansoori et al., 2020; Ravar et al., 2016; Surace et al., 2009; Xu et al., 2021). The modification was carried out to investigate the possibility of surface-modified liposomes with hyaluronic acid HA as a targeting ligand for colorectal cancer. The activation of HA and the formation of amide bonds are demonstrated in (Fig. 3).

Briefly, stock solutions of NHS, EDC and HA (1 mg/mL each) were prepared in deionized water. To activate hyaluronic acid (HA, 0.3 mg), NHS (0.1 mg) and EDC (0.3 mg) were added together and the mixture was left at room temperature (25 °C) overnight. After adjusting the DOPE concentration in each of the liposomal formulations to 1 mg/mL; 0.1 mL of activated HA was added to 0.9 mL of each of the blank liposome, REGO liposome, and CUR-liposome preparations. Furthermore, a DOPE control sample was also prepared at a concentration of 1 mg /ml and treated with activated HA in the same way as described above. These solutions were left at room temperature for 4 h. and then refrigerated to ensure the formation of the amide bond. Finally, a sample of each of the prepared HA-decorated liposomes was lyophilized and analyzed using Fourier transform infrared spectroscopy to determine the conformation of the amide bond formation.

2.2.3. Hyaluronic acid coating conformation using Fourier transform infrared (Ft-IR)

FT-IR analysis verified the conjugation of HA with DOPE in liposomal nanoparticles that was carried out using NHS/EDC to aid in the formation of amide bonds between the amine group of DOPE and the carboxyl group of HA (Mansoori et al., 2020).

To prepare the sample for FT-IR, a small amount of lyophilized liposome (about 0.1-2 %) was mixed with KBr powder, then the mixture was ground with mortar and pestle to produce a very fine powder, using the die-set together with the mini hand press, the mixture is compressed to form a transparent pellet ready to be inserted into the FT-IR.

Samples were prepared for DOPE alone, DOPE-HA, and HA alone to compare the FT-IR spectrum for each and to check for new amide bond formation, which should appear around 1635.6 cm^{-1}.

2.2.4. Particle size, polydispersity index (PDI), zeta potential (ZP) and morphology of liposomes

The particle size and ZP of the prepared liposomes were measured using a Malvern Zeta-sizer Nano Z® instrument (Malvern, Model ZEN3600 Ltd., UK). Deionized water was used to dilute all samples 200 times. A disposable cuvette was used for size measurement, while the prepared liposomal formulation was measured in reusable folded capillary cells (Model #DTS1061) with a dispersant refractive index of 1.33cP. At room temperature. all readings are expressed as an average of three consecutive measurements ± standard deviation (SD) (Lombardo & Kiselev, 2022).

To determine the liposomal morphology in terms of size, shape, and structure, Transmission Electron Microscopy (TEM, Morgagni 268 FEI, supported by the megaview soft imaging system) was used in the pathology and transmission electron microscopy unit, Faculty of Medicine, The University of Jordan, Amman, Jordan (Lombardo & Kiselev, 2022).

2.2.5. HPLC analysis

The concentration of REGO and CUR in all reference samples was directly analyzed using HPLC (Shimadzu Prominence-i LC-2030C 3D Plus) equipped with a Diode Array (PDA) Detector. LabSolutions CS Analysis Data System (Shimadzu Corporation, Kyoto, Japan), GraphPad Prism (RRID: SCR_002798) version 9.0.0 for Windows (GraphPad Software, Boston, MA USA, https://www.graphpad.com), and Microsoft Excel 2019 (RRID: SCR_016137) (https://www.microsoft.com/en-gb/) (Microsoft Corporation, Washington, USA) were used for statistical analysis and calculation of encapsulation efficiency (% EE). The chromatographic conditions were developed by in-house development using the following references with slight modifications (He et al., 1998; Hiserodt et al., 1996; Jayaprakasha et al., 2002; Lombardo & Kiselev, 2022).

The mobile phase consisted of the initial concentration of (A) acetonitrile and (B) 0.2 % aqueous acetic acid pH 3.2 in a ratio of (50:50 v/v) and with a gradient elution of (A: B) at 0, 5, 9, 10 minutes to be 50:50, 100:0, 100:0, 50:50 respectively, through a Hypersil GOLD™ C18 (Thermo-Fisher Scientific, USA, 250 × 4.6 mm, 5 µm), with a flow rate of 1.25 ml / min at oven temperature. The injection volume was 15 µL. The signals were captured from 200 to 450 nm and analyzed at 260 nm and 430 nm for the quantification of REGO and CUR, respectively.

Calibration curves for REGO and CUR were constructed using the following calibration curve equations (weighting factor 1/C):

$$REGO : f(x) = 53149.1x + 2872.90.$$

$$CUR : f(x) = 106698x + 4315.22.$$

2.2.5.1. Measurement of encapsulation efficiency (% EE). The incorporation of REGO and CUR in the bare-liposome and HA-liposome was quantitatively determined using HPLC. The % EE was calculated using

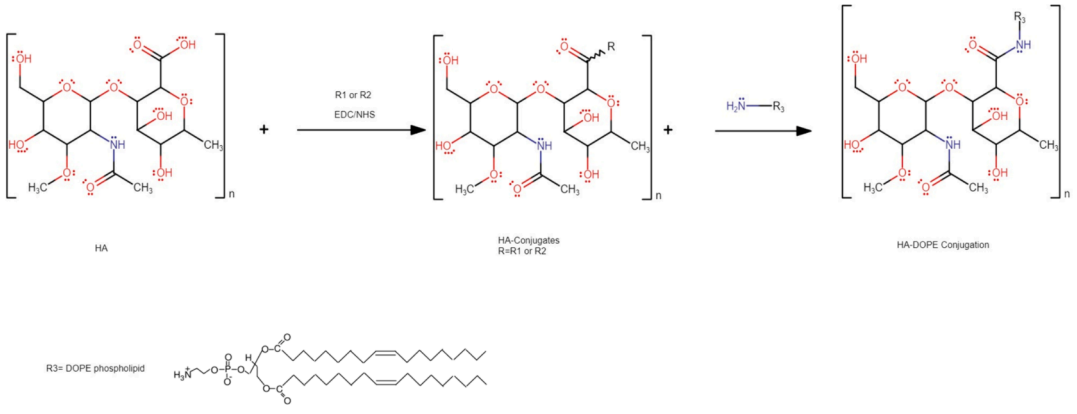

Fig. 3. Hyaluronic acid activation and conjugation with DOPE through the formation of amide bonds. Created with chem-space.com.

the following equation (Ravar et al., 2016; Xu et al., 2021):

$$\%EE = (Amountofdrugcaught)/(Totalamountofdrug) \times 100 \quad (1)$$

The liposome encapsulation efficiency was calculated using the disruption method. Briefly, 10 µl of drug-loaded liposomes were mixed with 100 µl of acetonitrile while vortexing to disrupt the liposome and analyze the total amount of drug (free and encapsulated), and then 100 µl of 50 % aqueous methanol was added, the samples were placed in a centrifuge (5000RPM) for 10 min to ensure the precipitation of the disrupted liposomal lipids. The supernatant was collected and analyzed (n = 3) using HPLC.

To calculate the amount of drug alone we must determine first the amount of free drug out of the liposome(un-trapped), 200 µl of the liposomal formula was placed in an Eppendorf tube and centrifuged at 15000 RPM for 30 min to settle the drug loaded liposomes. The supernatant (50 µl) was taken and diluted up to 2 ml with 50 % aqueous methanol (dilution factor 40) to assess the presence of free drug using HPLC (n = 3).

The total and free drug amounts were calculated by plotting the Area Under the Curve (AUC) obtained via HPLC in the calibration equation and multiplying the values by the dilution factor. The free drug's value was then subtracted from the total drug value to determine the amount of entrapped drug. Finally, the values obtained were then incorporated into the formula to calculate the % EE (Ravar et al., 2016; Xu et al., 2021).

2.2.6. In vitro release

To assess the rate of CUR and REGO release from nanoparticles, the dialysis bag diffusion technique was used. Briefly, 100 µl of each prepared liposomal sample in addition to the free drug was placed individually in a dialysis tube with a diffusion surface area of 0.5027 cm^2 (molecular weight cut-off points (MWCO); 10 kDa.) and immersed in 2 ml of PBS (157.9 mM, pH 7.4) in a closed apparatus to prevent evaporation. The release system was set at 37 °C and 100 rpm in a shaker incubator. At predetermined time intervals (2, 4, 6, 48, 72, and 96 h), aliquots of the release medium were collected from each sample (100 µL) and substituted with fresh buffer solution. The concentration of CUR and REGO in the collected samples is analyzed using HPLC as it was mentioned earlier (Mansoori et al., 2020). The cumulative amount of CUR and REGO released from the liposomal formulations was then calculated based on the concentration measured at each time point using the following equation to calculate the % leak:

$$\%leak = (cumulativeamountleaked)/(totalamountinliposomes) \times 100\% \quad (2)$$

Finally, the release profiles of CUR and REGO were plotted as cumulative release (%) versus time (hours) to visualize the release kinetics over the previous time points.

2.2.7. Cell viability assay

The 3-(4,5 dimethyl-2-thiazolyl)-2,5-diphenyltetrazolium bromide (MTT) assay was used to measure cell viability after incubation with free REGO, free CUR, REGO-LIPO, CUR-LIPO, REGO-LIPO-HA, CUR-LIPO-HA (Chacon et al., 1997; Plumb, 1999; van Meerloo et al., 2011). In brief, 5.5×10^3 HT-29 cells in passage 20 were seeded in each well of a 96-well plate. Cells were treated with different concentrations starting from 190 µM of free REGO, CUR and their Nano formulations. After 72 h, 10 µL of MTT solution was added to each well. The incubation medium was replaced with 100 µL of DMSO after 4 h. Then the absorption of the plates was read at a wavelength of 570 nm using a multimode reader (BioTek, USA).

All experiments were carried out in triplicate. The IC_{50} (concentration resulting in 50 % inhibition of cell growth) has been graphically calculated from the concentration viability curve using GraphPad Prism (RRID: SCR_002798) version 9.0.0 for Windows, GraphPad Software, Boston, Massachusetts, USA, https://www.graphpad.com.

3. Results

3.1. Preparation and Characterization of liposomal nanoparticles

3.1.1. Size, polydispersity index (PDI) and zeta potential (ZP)

The particle size and zeta potential of the prepared liposomes were measured using a Malvern Zetasizer Nano Z® instrument and all parameters obtained were expressed as mean ± SD.

As shown in the following data, the average particle sizes of regorafenib-loaded plain liposomes and those decorated with HA were 144.00 ± 0.78 nm and 140.77 ± 1.64 nm, with a PDI value of 0.24 ± 0.01 and 0.23 ± 0.02 respectively (Fig. 4 a-b), while the average particle size of curcumin-loaded plain liposomes and liposomes decorated with HA was 140.10 ± 2.46 nm and 164.53 ± 15.13 nm with a PDI value of 0.23 ± 0.02 and 0.22 ± 0.01 respectively (Table 2) and (Fig. 4 c d).

The average surface charge of the blank liposome was −55.37 ± 16.02 mV, for the regorafenib loaded plain liposomes and HA-decorated ZP values decorated with HA were −48.13 ± 13.23 and −61.3 ± 9.91 mV, respectively. At the same time, the mean ZP of curcumin-loaded plain liposomes and HA-decorated liposomes were −52.2 ± 2.96 and −73.43 ± 12.52 mV respectively (Table 2).

3.1.2. Transmission electron microscopy (TEM) of liposomes

TEM was used to analyze the morphology of the prepared liposomal nanoparticles (Ruozi et al., 2011). The zeta sizer values and the resulting TEM size ranges were similar. In contrast to TEM, which uses transmitted electrons to measure the displayed area diameter of a particle in a fixed position (solid sample) with no hydration layer, the zeta sizer uses the process of dynamic light scattering to measure the hydrodynamic dimension of scattered liposomes within a solution, incorporating the solvation layers while they navigate within the effect of Brownian motion. Nevertheless, Consequently, both tactics work well together (Ravar et al., 2016). The formulated liposomes were spherical, monodispersed and free of significant aggregation or fusion (Fig. 5a).

3.1.3. % EE encapsulation efficiency for the bare and HA-Coated liposomal preparations.

The average value of % EE was found to be 99.22 %±0.29 and 99.87 %±0.17 for the bare-REGO liposome and the HA-REGO liposomal nanoparticles, respectively, while these values were calculated to be 98.9 %±0.18 and 97.49 %±0.2 for the bare CUR liposome and HA-CUR-liposomal nanoparticles respectively (Table 2) and (Fig. 5b).

3.1.4. Drug release

The maximum percent leak after 96 h of incubation was 0.9, 0.72, and 0.73 % for free REGO, REGO-LIPO, and REGO-LIPO-HA, respectively. In the case of free CUR, CUR-LIPO, and CUR-LIPO-HA the percentage leaks were 0.2, 1, and 0 % respectively (Fig. 6).

3.2. Effect of liposomal formulation on colorectal cancer cell line

The MTT assay was used to assess how free REGO, free CUR, REGO-LIPO, CUR-LIPO, REGO-LIPO-HA, and CUR-LIPO-HA nanoparticles affected the viability of HT29 cells. At 72 h, a significant decrease in cell viability was observed in (Fig. 7). For the 72-hour incubation period with HT29 cancer cells, the IC_{50} of free REGO, free CUR, REGO-LIPO, CUR-LIPO, REGO-LIPO-HA and CUR-LIPO-HA was 20.17 ± 0.78, 64.4 ± 0.33, 224.8 ± 0.06, 49.66 ± 0.22, 73.66 ± 0.6, and 27.86 ± 0.49 µM respectively (Table 3).

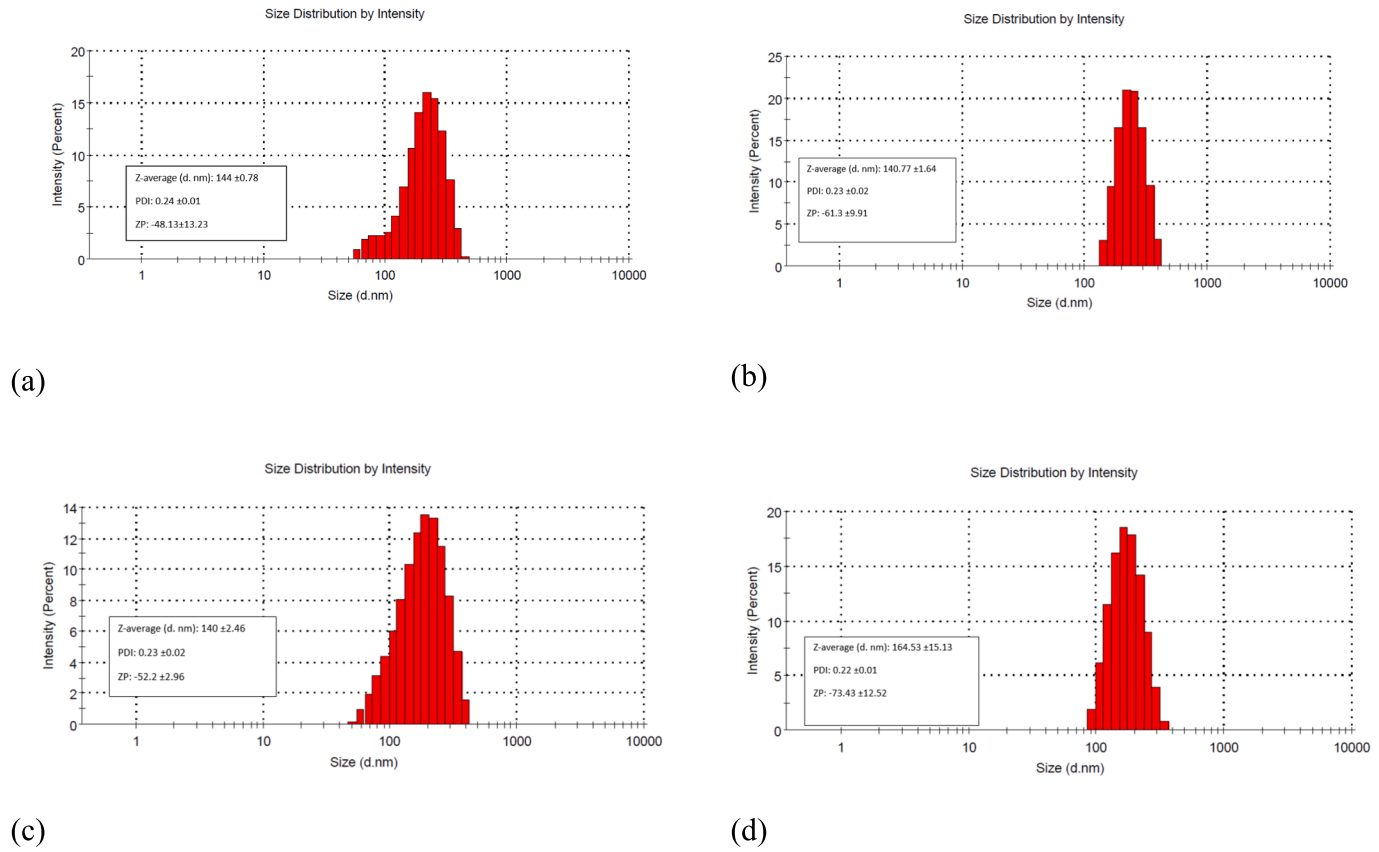

Fig. 4. Average particle size distribution obtained by DLS. (a) REGO-LIPO, (b) REGO-LIPO-HA, (c) CUR-LIPO, and (d) CUR-LIPO-HA. DLS, dynamic light scattering; HA, hyaluronic acid; REGO, regorafenib; CUR, curcumin; LIPO, liposome. The results are presented as mean ± SD of triplicate measurements.

Table 2
Characterization of plain and hyaluronic acid-decorated liposomal formulations with REGO and CUR.

Formulation	Size (nm)	PDI	Zeta potential (mV)	Total drug concentration (μg/mL)	Concentration of entrapped drug (μg/mL)	Encapsulation efficiency (%)
Blank-LIPO	339.3 ± 5.62	0.44 ± 0.03	−59.77 ± 0.31	–	–	–
REGO-LIPO	144.0 ± 0.78	0.24 ± 0.01	−48.13 ± 13.23	263.99 ± 3.14	261.93 ± 3.73	99.22 ± 0.29
REGO-LIPO-HA	140.77 ± 1.64	0.23 ± 0.02	−61.3 ± 9.91	206.42 ± 2.53	206.15 ± 2.4	99.87 ± 0.17
CUR-LIPO	140.10 ± 2.46	0.23 ± 0.02	−52.2 ± 2.96	221.67 ± 6.82	219.23 ± 7.03	98.90 ± 0.18
CUR-LIPO-HA	164.53 ± 15.13	0.22 ± 0.01	−73.43 ± 12.52	100.79 ± 7	98.26 ± 7	97.49 ± 0.2

4. Discussion

4.1. Preparation and Characterization of liposomal nanoparticles

4.1.1. Hyaluronic acid conjugation conformation using Fourier-Transform infrared spectroscopy (Ft-IR)

The thin layer film hydration method was used to prepare the liposomal nanoparticles, and later the surface was modified with an active targeting ligand (HA) for colorectal cancer cells. As stated in the methodology earlier, EDC was used to enable the conjugation of HA to DOPE in the liposomal nanoparticles, which helped to form the amide link between the two molecules. FT-IR spectroscopy was used to check amide bond formation (Fig. 8).

Using FT-IR to check the spectrum for DOPE alone, DOPE-HA, and HA alone (Fig. 8, a), we can observe the formation of a new peak with the DOPE-HA spectrum at 1635.6 cm^{-1}, which was not observed in the spectrums for either the DOPE or the HA alone. This infrared (IR) band represents the formation of an –CO-NH- (amide bond) between HA and DOPE. It was used to confirm bond formation. Therefore, the presence of these bands in the IR spectra of HA and DOPE demonstrated the formation of the DOPE–HA conjugation. This outcome is consistent with numerous previous studies demonstrating the conjugation of HA to DOPE through the formation of covalent amide bonds (Hayward et al., 2016; Mansoori et al., 2020).

On the basis of these data, we coated the liposomal formulations of regorafenib, curcumin, and blank unloaded liposomes (REGO-LIPO-HA, CUR-LIPO-HA, BLANK-LIPO-HA). Similarly, the FT-IR of the formulations (Fig. 8, b) showed the same peak at 1635 cm^{-1}, indicating amide bond formation as well, hence a successful coating.

4.1.2. Size, polydispersity index (PDI) and zeta potential (ZP)

According to the literature, the fate of liposomal nanoparticles in vivo fate can be affected by several factors, including their vascular size and surface charge. The reticuloendothelial system (RES), which is mainly composed of the liver and spleen, tends to quickly eliminate liposomes larger than 200 nm. In contrast, renal clearance may be possible for liposomes smaller than 70 nm. Liposomes in the 70–200 nm range can prolong their circulation time and enhance their accumulation in tumor tissues by striking a balance between avoiding rapid RES clearance and renal clearance.

The literature indicates that the vascular size and surface charge of liposomal nanoparticles can have an impact on their in vivo fate.

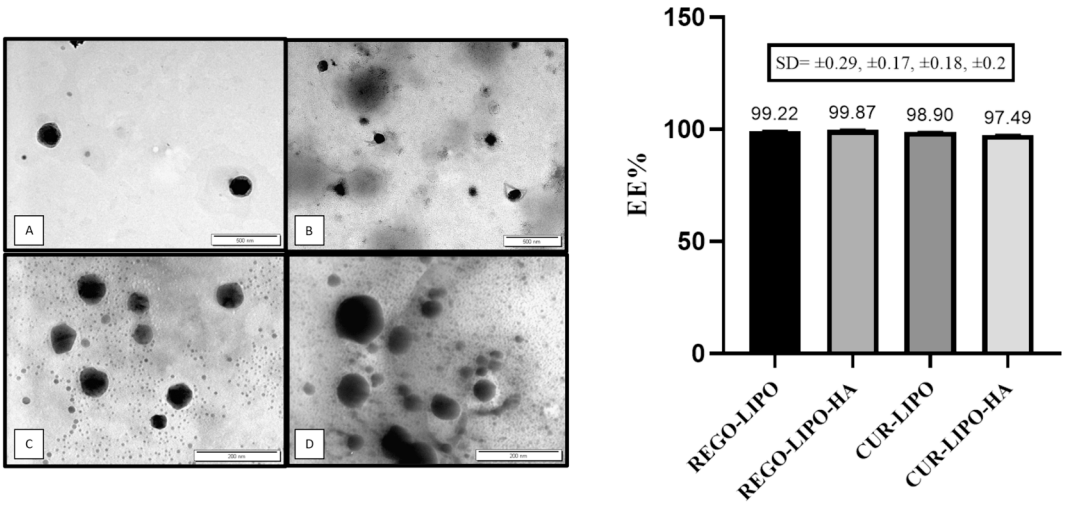

Fig. 5. Liposomal morphology and encapsulation efficiency. (a) Transmission electron microscopy image of (A) REGO-LIPO, (B) REGO-LIPO-HA, (C) CUR-LIPO, (D) CUR-LIPO-HA. Scale bar: 200 nm, 500 nm. (b) The % encapsulation efficiency values of regorafenib and curcumin's HA-coated and uncoated liposomal formulations with the results presented as mean ± SD of triplicate measurements.

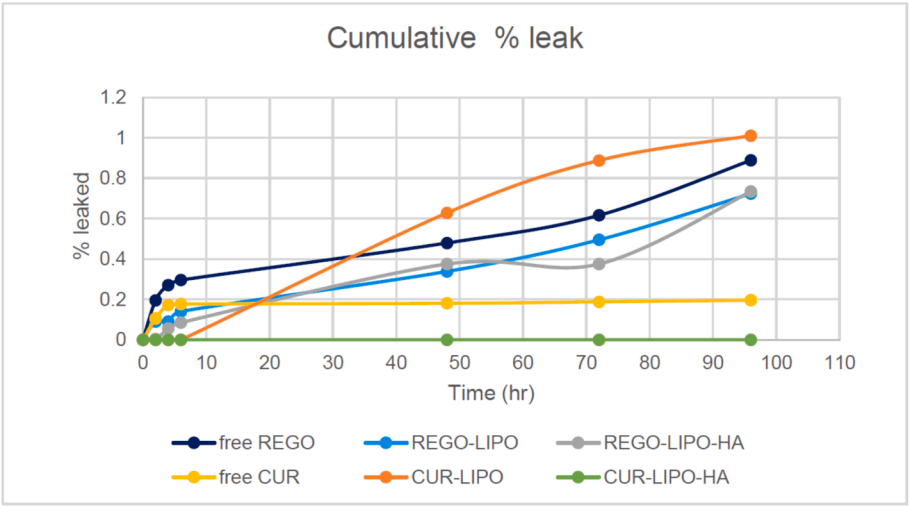

Fig. 6. Schematic diagram of in vitro release of REGO and CUR from bare-LIPO and LIPO-HA compared with the free drug form at pH 7.4 represented as % leaked at different time points up to 96 h.

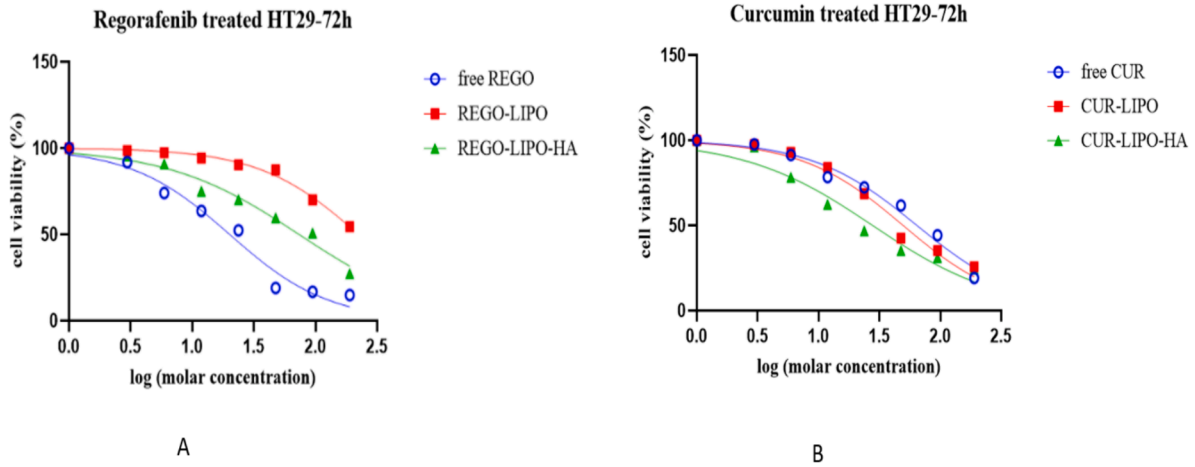

Fig. 7. Relative cell viability of HT29 colorectal cancer cells treated with Free REGO, Free CUR, REGO-LIPO, CUR-LIPO, REGO-LIPO-HA and CUR-LIPO-HA for 72 h (cell viability % vs logarithmic molar concentration (μM)). The results are presented as mean ± SD of the measurements in triplicate.

Table 3
Relative cell viability of HT29 colorectal cancer cells treated with Free REGO, Free CUR, REGO-LIPO, CUR-LIPO, REGO-LIPO-HA and CUR-LIPO-HA for 72 h.

Column	Free REGO	Free CUR	REGO-LIPO	CUR-LIPO	REGO-LIPO-HA	CUR-LIPO-HA
IC_{50}(μM) ± SD	20.17 ± 0.78	64.4 ± 0.33	224.8 ± 0.06	49.66 ± 0.22	73.66 ± 0.6	27.86 ± 0.49
Log IC_{50}	1.31	1.81	2.35	1.7	1.87	1.45
Degrees of Freedom	6	6	6	6	6	6
R squared	0.97	0.98	0.99	0.98	0.97	0.95

Liposomes larger than 200 nm are rapidly eliminated by the reticuloendothelial system (RES), which consists mainly of the liver and spleen. In contrast, liposomes smaller than 70 nm might be subject to renal clearance. Liposomes in the 70–200 nm range have the ability to balance renal clearance and RES clearance, allowing them to maximize their concentration in tumor tissues and prolong their circulation time (Mansoori et al., 2020; Ravar et al., 2016).

Additionally, liposomes ranging in size from 70 to 200 nm showed an improved impact of permeability and retention (EPR) (Raju et al., 2023). This finding implies that nanoparticles in this size range may passively collect in tumor tissues, since solid tumors generally have leaky vasculature and inadequate lymphatic drainage. Liposomes that are in circulation for extended periods are more likely to find their way into tumor tissues and begin to accumulate there (Guimares et al., 2021; Raju et al., 2023; William et al., 2020).

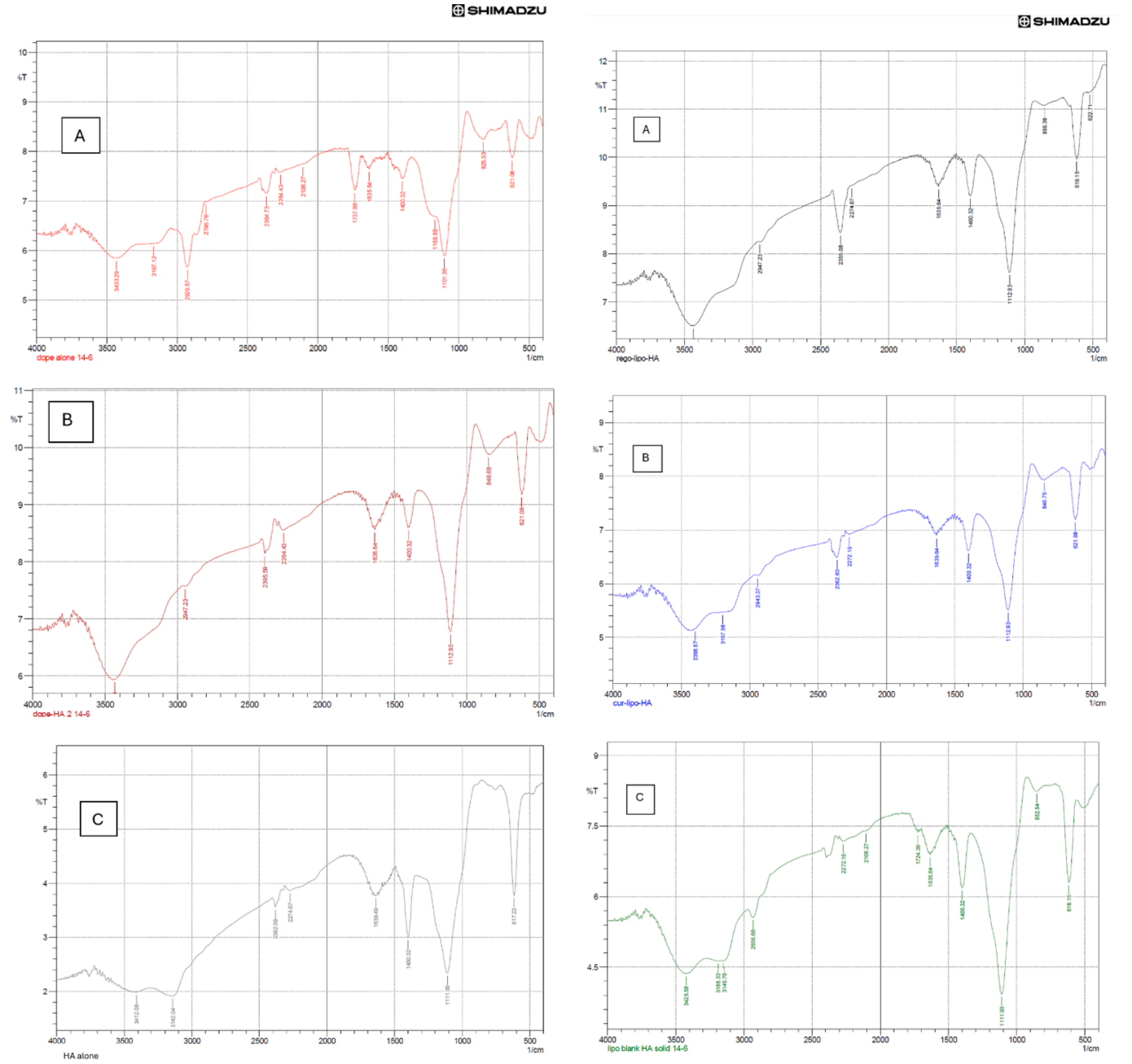

Fig. 8. FT-IR spectrum; transmittance (%T) against the wavenumber (1/cm). [a]: (A) DOPE-HA, (B) DOPE, and (C) HA. [b]: (A) REGO-LIPO-HA, (B) CUR-LIPO-HA, and (C) BLANK-LIPO-HA. The peak at 1635 cm^{-1} represents the amide bond formation.

Additionally, previous research also suggested that particle size plays a crucial role in passive targeting by allowing particles to pass through the blood vessel gaps in tumors. Poor lymphatic drainage and small particles (200 nm) below the pore size of leaky vessels create ideal conditions for the accumulation and localization in the tumor area (Danaei et al., 2018; Ravar et al., 2016).

As we can observe from these results in both cases, according to a study by (Ravar et al., 2016), the size obtained size and PDI are considered acceptable and follow the CQA which are crucial for its activity in the tumor microenvironment, and for prolonged blood circulation which is confirmed by our findings in both cases of the coated and the uncoated formulations, and in turn is in line with the reported research (Ravar et al., 2016). All prepared drug-loaded liposomal formulations gave an acceptable average particle size compared to the blank unloaded liposomal formula (339.3 ± 5.62 nm, PDI 0.44 ± 0.03) which can indicate that regorafenib and curcumin as a lipophilic active moieties, contribute to the stability of the liposomes once loaded into the lipid bilayer. The hyaluronic acid coating stabilizes the liposomal formulation and gives a more uniform size according to the results mentioned in (Table 2) and (Fig. 4).

The ZP is an essential factor that has a direct bearing on the stability of the liposomal dispersion. It has been generally accepted that if ZP values fall between −30 and +30 mV, liposomal particles can aggregate due to the insufficient electric repulsion between them (Barbălată et al., 2021; Tefas et al., 2017). These obtained values are considered accepted and preferred with the aim of stabilizing the liposomal nanoparticles and agree with the CQA of the liposomal preparation (Barbălată et al., 2021). Surface functionalization of liposomal nanoparticles with HA was confirmed by these general findings (Hayward et al., 2016).

4.1.3. Transmission electron microscopy (TEM) of liposomes

The samples used for the TEM analysis were of the same batch and treated similarly by extruding the sample before coating and then the coating step followed by TEM testing to efficiently compare the difference that comes with the coating step in both drug cases. Formulations decorated with HA seem to have a slightly larger diameter compared to uncoated liposomes, and this is because the hydrophilic molecule HA is reported to be able to absorb water and expand over its original size in an aqueous environment, as seen by (Ravar et al., 2016). The conjugation of HA molecules on the liposome's exterior is what causes its hydrodynamic size to rise.

4.1.4. % EE encapsulation efficiency for the bare and HA-Coated liposomal preparations.

According to several previous studies (Mansoori et al., 2020), the findings revealed that there was no significant difference between EE for bare and HA-decorated liposomes for REGO and CUR (P value > 0.05). The high value of encapsulation efficiency in both cases is related to the high lipophilicity of both REGO (log P = 4.5) and CUR (log P ~ 3.0) respectively (Priyadarsini, 2014), in addition to the lipid composition of the liposomal formulas (saturation level and transition temperature (Tm)). for example, DPPC is a saturated lipid with Tm = 41 °C, and DPPG Tm = 41 °C, this can increase% EE and reduce drug leakage from the liposome (Barbălată et al., 2021).

These results are in line with the CQAs of liposomal formulas to reduce the loss mentioned in the literature (Barbălată et al., 2021), indicating that the EE value should be above 50 %. Furthermore, a higher % EE can reduce the amount of drug leaked from the actively targeted liposome, which in turn reduces side effects resulting from the high amount of free drug in the bloodstream, which also ensures that most of the drug will reach the targeted tumor (Barbălată et al., 2021; Kang et al., 2023). In addition to the possibility of using this system as a depot to allow long blood circulation of the liposomal formula, which is also ensured by the negative ZP presented previously (Ravar et al., 2016).

4.1.5. Drug release

Regarding the in vitro release test, the aim was to ensure that the drug would remain loaded into the liposome throughout its journey in the bloodstream and to further improve the cellular activity of the liposomal formula, especially the actively targeted one that was seen in the cell cytotoxicity test that will be demonstrated later, being dependent on the liposomal formulation (endocytosis) rather than the free drug. This was confirmed in the following results (Fig. 6), showing that the cumulative % leakage of the drug from all formulations (incubated for 96 h at pH 7.4) was less than 1 %, which means that the drug remains loaded into the liposome during this period due to its lipophilic properties and the stability of the liposome as previously demonstrated.

The low cumulative percentage of drug leakage (<1 %) of the drug from all formulations during 96-hour incubation at pH 7.4 demonstrates the remarkable stability and efficacy of the liposomal formulations. This finding suggests that liposomes can maintain their structural integrity and drug encapsulation efficiency for an extended period under physiological conditions. Such stability reduces premature drug release by keeping the majority of the drug encapsulated within the liposomes during circulation, reducing systemic side effects and increasing drug delivery to the target site. Furthermore, the low leakage rate implies a sustained drug release profile, which may lead to improved therapeutic outcomes (Ye et al., 2014).

This also indicates that the observed activity of the liposomal formulation is due to the encapsulated liposome and its endocytosis to the cancer cell. An additional observation was with respect to the HA-decorated formulas compared to the uncoated ones, it seems that HA has prolonged the release of the drugs in the coated formulas, and this can be clearly seen in the case of CUR-LIPO-HA.

This is possibly attributed to the hydrophilic exterior conjugation of HA molecules on the liposomal surface, resulting in reduced permeability and bilayer fluidity (Ravar et al., 2016), It was observed that the HA coating on the liposome surface extended drug release. Furthermore, the dense hydrophilic matrix created by the HA molecules surrounding the liposomes slows the release of hydrophobic active moieties (regorafenib and curcumin).

4.2. Effect of lipid formulation on colorectal cancer cell line

According to the results of the MTT assay in (Table 3) and (Fig. 7), compared to REGO-LIPO (IC_{50} 224.8 ± 0.06 μM); REGO-LIPO-HA (IC_{50}73.66 ± 0.6 μM) demonstrated a greater reduction in cell viability. The HA-coated liposomal formulation actively targeted in both drug cases showed a greater reduction in HT29 cell viability compared to the non-targeted bare liposomal formulations.

A similar observation was made with CUR-LIPO-HA (IC_{50} 27.86 ± 0.49 μM) in comparison to CUR-LIPO (IC_{50} 49.66 ± 0.22 μM). The MTT assay findings showed that both nanoparticles significantly decreased cell viability when compared to control cells.

In general, REGO-LIPO-HA nanoparticles outperformed REGO-LIPO in terms of cytotoxicity to HT29 cells, while the free REGO formulation demonstrated superior activity compared to both liposomal formulations. Regarding curcumin formulations, CUR-LIPO-HA nanoparticles outperformed CUR-LIPO and free CUR (IC_{50} 64.4 ± 0.33 μM).

These results are in line with research on cellular uptake, which demonstrated that HA-decorated liposomes were absorbed more efficiently by HT29 cancer cells than bare liposomes (Eliaz & Szoka, 2001; Tiantian et al., 2014). HA surface functionalization enhances the targeting of colorectal cancer cells via CD44 receptors, improving drug uptake and efficacy while reducing off-target effects. This specificity minimizes systemic toxicity and maximizes therapeutic benefit. Additionally, HA-functionalized liposomes exhibit prolonged retention in tumor tissues, potentially improving sustained therapeutic effects (Hayward et al., 2016).

Furthermore, it was discovered that HA-decorated liposome

nanoparticles had a higher affinity for binding to CD44 receptors, which is overexpressed by HT29 colorectal cancer cell lines (Najafi et al., 2023). As a result, HA-decorated liposomes can bind to CD44 receptors and internalize into cells through CD44 receptor-mediated endocytosis. This increased internalization leads to higher intracellular drug concentrations and subsequently to greater cytotoxic effects on HT29 cells (Hayward et al., 2016; Zhao et al., 2014). HA surface functionalization enhances the targeting of colorectal cancer cells via CD44 receptors, improving drug uptake and efficacy while reducing off-target effects. This specificity minimizes systemic toxicity and maximizes therapeutic benefit. Furthermore, HA-functionalized liposomes exhibit prolonged retention in tumor tissues, potentially improving sustained therapeutic effects (Elliott et al., 2014; Machado et al., 2022; Manzari-Tavakoli et al., 2024).

However, bare liposomes could also enter cells through passive targeting (nonspecific endocytosis) (Eliaz & Szoka, 2001; Hayward et al., 2016; Tiantian et al., 2014; Zhao et al., 2014). It can be argued that the active targeting of REGO and CUR liposomes to HA of HT29 cancer cells led to higher cytotoxicity and more selective targeting of HT29 cancer cells due to HA binding to CD44 receptors.

5. Conclusions

In conclusion, a passive and actively targeted liposomal formulation was developed to improve the safety and efficacy of the anticancer agents regorafenib and curcumin against colorectal cells. Actively targeted liposomes with HA surface modification were created to target the CD44 receptor in colorectal cancer cells. The prepared liposomes had acceptable CQA, including small particle size, PDI value, zeta potential −30 mv, and a high % EE. Additionally, compared to bare liposomal nanoparticles, the HA-decorated drug delivery systems did not show significant differences in the % EE. These CQAs, along with the HA targeting moiety, made it easier for HT29 cells to absorb liposomes by CD44 receptor-mediated endocytosis. Compared to free drug and conventional liposomes, actively targeted liposomes had improved cytotoxic activity due to their superior uptake and this was observed with curcumin-loaded HA-decorated liposomes especially.

In vitro release assay, as well as % EE indicates that the liposomes contain ~98 % of the loaded drug. The percentage of leakage of liposomes (both coated and uncoated) was found to be less than 1 % in all prepared formulations. This suggests that liposomes are stable at physiological pH and body temperature. Furthermore, by checking the % leak profile for each formulation, we can observe that the HA coating extends the drug release profile from the coated liposomes in comparison to the uncoated ones. This indicates that HA conjugation can result in a longer time for the drugs to be released from the HA-coated formulas, as demonstrated by the CUR-LIPO-HA case.

Additionally, the MTT assay showed encouraging results, particularly when the IC50 values of the coated formulations were compared with those of the free drug or uncoated liposomes, as was the case with curcumin. The CUR-LIPO-HA IC50 value was IC50 27.86 ± 0.49 μM. IC50 decreases when we coat the formulation to improve liposome selectivity, which suggests a decrease in the systematic cytotoxicity and demonstrating an increase in efficacy. These findings suggest that REGO-LIPO-HA and CUR-LIPO-HA may be promising tumor-targeted drug delivery systems for improving the therapeutic effect in the treatment of colorectal cancer and metastatic colorectal cancer cells while improving the safety and efficacy of cytotoxic agents especially regorafenib. To validate our findings, we suggest at this time conducting an in vivo test on an animal model to evaluate the safety and effectiveness of the liposome. This will provide insights into the formulation's performance in a more complex biological environment and its potential applications in clinical settings. In addition, mechanistic studies are based on the examination of colorectal cancer cells and the fundamental mechanisms of action of liposomal formulations targeted at HA. This could involve researching intracellular trafficking, cellular uptake pathways, and the effects on important signaling pathways related to the development and prognosis of cancer. It is also supported by the comparison conducted between coated and the uncoated liposomes in terms of cytotoxicity.

Funding

This project was supported by Deanship of Higher Education and Research, Al-Ahliyya Amman University, Amman, Jordan.

CRediT authorship contribution statement

Sewar G. Shnaikat: Conceptualization, Data curation, Formal analysis, Investigation, Methodology, Software, Validation, Visualization, Writing – original draft, Writing – review & editing. **Ashok K Shakya:** Conceptualization, Data curation, Formal analysis, Funding acquisition, Investigation, Methodology, Project administration, Resources, Software, Supervision, Validation, Visualization, Writing – original draft, Writing – review & editing. **Sanaa K. Bardaweel:** Conceptualization, Formal analysis, Investigation, Methodology, Supervision, Visualization, Writing – original draft, Writing – review & editing.

Declaration of Competing Interest

The authors declare that they have no known competing financial interests or personal relationships that could have appeared to influence the work reported in this paper.

Acknowledgement

The authors wish to thank the Deanship, Faculty of Pharmacy, and the Dean of Research and Higher Education, Al-Ahliyya Amman University, Amman, Jordan, for providing necessary facilities.

Appendix A. Supplementary material

Supplementary material to this article can be found online at https://doi.org/10.1016/j.jsps.2024.102099.

References

Amekyeh, H., Alkhader, E., Sabra, R., Billa, N., 2022. Prospects of curcumin nanoformulations in cancer management. Molecules 27 (2), Article 2. https://doi.org/10.3390/molecules27020361.

Andra, V.V.S.N.L., Pammi, S.V.N., Bhatraju, L.V.K.P., Ruddaraju, L.K., 2022. A Comprehensive Review on Novel Liposomal Methodologies, Commercial Formulations, Clinical Trials and Patents. BioNanoScience 12 (1), 274–291. https://doi.org/10.1007/s12668-022-00941-x.

Barbălată, C.I., Porfire, A.S., Sesarman, A., Rauca, V.-F., Banciu, M., Muntean, D., Ştiufiuc, R., Moldovan, A., Moldovan, C., Tomuță, I., 2021. A screening study for the development of simvastatin-doxorubicin liposomes, a Co-formulation with future perspectives in colon cancer therapy. Pharmaceutics 13 (10), 1526. https://doi.org/10.3390/pharmaceutics13101526.

Bardania, H., Jafari, F., Baneshi, M., Mahmoudi, R., Ardakani, M.T., Safari, F., Barmak, M.J., 2023. Folic acid-functionalized albumin/graphene oxide nanocomposite to simultaneously deliver curcumin and 5-fluorouracil into human colorectal cancer cells: an *in vitro* study. Biomed Res. Int. 2023, e8334102.

Biller, L., Schrag, D., 2021. Diagnosis and treatment of metastatic colorectal cancer: a review. JAMA 325, 669–685. https://doi.org/10.1001/jama.2021.0106.

Chacon, E., Acosta, D., & Lemasters, J. J. (1997). *Primary Cultures of Cardiac Myocytes as In Vitro Models for Pharmacological and Toxicological Assessments*. 209–223. Doi: 10.1016/B978-012163390-5.50010-7.

Chen, Y., Du, Q., Guo, Q., Huang, J., Liu, L., Shen, X., Peng, J., 2019. A W/O emulsion mediated film dispersion method for curcumin encapsulated pH-sensitive liposomes in the colon tumor treatment. Drug Dev. Ind. Pharm. 45 (2), 282–291. https://doi.org/10.1080/03639045.2018.1539099.

Chen, Y., Wang, Z., Wang, X., Su, M., Xu, F., Yang, L., Jia, L., Zhang, Z., 2022. Advances in antitumor nano-drug delivery systems of 10-hydroxycamptothecin. Int. J. Nanomed. 17, 4227–4259. https://doi.org/10.2147/IJN.S377149.

Crona, D.J., Keisler, M.D., Walko, C.M., 2013. Regorafenib: A novel multitargeted tyrosine kinase inhibitor for colorectal cancer and gastrointestinal stromal tumors.

Ann. Pharmacother. 47 (12), 1685–1696. https://doi.org/10.1177/1060028013509792.
Danaei, M., Dehghankhold, M., Ataei, S., Hasanzadeh Davarani, F., Javanmard, R., Dokhani, A., Khorasani, S., Mozafari, M.R., 2018. Impact of particle size and polydispersity index on the clinical applications of lipidic nanocarrier systems. Pharmaceutics 10 (2), 57. https://doi.org/10.3390/pharmaceutics10020057.
Dhillon, S., 2018. Regorafenib: a review in metastatic colorectal cancer. Drugs 78 (11), 1133–1144. https://doi.org/10.1007/s40265-018-0938-y.
Eliaz, R.E., Szoka, F.C., 2001. Liposome-encapsulated doxorubicin targeted to CD44: a strategy to kill CD44-overexpressing tumor cells. Cancer Res. 61 (6), 2592–2601.
Elliott, V.A., Rychahou, P., Zaytseva, Y.Y., Evers, B.M., 2014. Activation of c-Met and upregulation of CD44 expression are associated with the metastatic phenotype in the colorectal cancer liver metastasis model. PLoS One 9 (5), e97432.
Ettrich, T.J., Seufferlein, T., 2018. Regorafenib. *recent results in cancer research. fortschritte der krebsforschung*. Progres. Dans. Les. Recherches Sur Le Cancer 211, 45–56. https://doi.org/10.1007/978-3-319-91442-8_3.
Fazli, B., Irani, S., Bardania, H., Moosavi, M.-S., Rohani, B., 2022. Prophylactic effect of topical (slow-release) and systemic curcumin nano-niosome antioxidant on oral cancer in rat. BMC Complement. Med. Therapies 22 (1), 109. https://doi.org/10.1186/s12906-022-03590-5.
Guimarães, D., Cavaco-Paulo, A., Nogueira, E., 2021. Design of liposomes as drug delivery system for therapeutic applications. Int. J. Pharm. 601, 120571 https://doi.org/10.1016/j.ijpharm.2021.120571.
Gunter, M.J., Alhomoud, S., Arnold, M., Brenner, H., Burn, J., Casey, G., Chan, A.T., Cross, A.J., Giovannucci, E., Hoover, R., Houlston, R., Jenkins, M., Laurent-Puig, P., Peters, U., Ransohoff, D., Riboli, E., Sinha, R., Stadler, Z.K., Brennan, P., Chanock, S. J., 2019. Meeting report from the joint IARC-NCI international cancer seminar series: a focus on colorectal cancer. Annals of Oncology: Offi. J. Eur. Soc. Med. Oncol. 30 (4), 510–519. https://doi.org/10.1093/annonc/mdz044.
Hayward, S.L., Wilson, C.L., Kidambi, S., 2016. Hyaluronic acid-conjugated liposome nanoparticles for targeted delivery to CD44 overexpressing glioblastoma cells. Oncotarget 7 (23), 34158–34171. https://doi.org/10.18632/oncotarget.8926.
He, X.-G., Lin, L.-Z., Lian, L.-Z., Lindenmaier, M., 1998. Liquid chromatography–electrospray mass spectrometric analysis of curcuminoids and sesquiterpenoids in turmeric (Curcuma longa). J. Chromatogr. A 818 (1), 127–132. https://doi.org/10.1016/S0021-9673(98)00540-8.
Hewlings, S.J., Kalman, D.S., 2017. Curcumin: a review of its' effects on human health. Foods 6 (10), 92. https://doi.org/10.3390/foods6100092.
Hiserodt, R., Hartman, T.G., Ho, C.-T., Rosen, R.T., 1996. Characterization of powdered turmeric by liquid chromatography-mass spectrometry and gas chromatography-mass spectrometry. J. Chromatogr. A 740 (1), 51–63. https://doi.org/10.1016/0021-9673(96)00103-3.
Ho, M.J., Park, D.W., Kang, M.J., 2023. Design of novel tricaprylin-incorporated multi-layered liposomal system for skin delivery of ascorbic acid with improved chemical stability. Pharmaceuticals 16 (1), 121. https://doi.org/10.3390/ph16010121.
Jayaprakasha, G.K., Rao, J.M., L., & Sakariah, K. K., 2002. Improved HPLC method for the determination of curcumin, demethoxycurcumin, and bisdemethoxycurcumin. J. Agric. Food Chem. 50 (13), 3668–3672. https://doi.org/10.1021/jf025506a.
John, R., Monpara, J., Swaminathan, S., Kalhapure, R., 2024. Chemistry and art of developing lipid nanoparticles for biologics delivery: focus on development and scale-up. Pharmaceutics 16 (1), 131. https://doi.org/10.3390/pharmaceutics16010131.
Kang, C., Wang, J., Li, R., Gong, J., Wang, K., Wang, Y., Wang, Z., He, R., Li, F., 2023. Smart targeted delivery systems for enhancing antitumor therapy of active ingredients in traditional chinese medicine. Molecules (Basel, Switzerland) 28 (16), 5955. https://doi.org/10.3390/molecules28165955.
Kumar, R., Harilal, S., Carradori, S., Mathew, B., 2021. A comprehensive overview of colon cancer- a grim reaper of the 21st century. Curr. Med. Chem. 28 (14), 2657–2696. https://doi.org/10.2174/0929867327666201026143757.
Leonenko, Z.V., Finot, E., Ma, H., Dahms, T.E.S., Cramb, D.T., 2004. Investigation of temperature-induced phase transitions in DOPC and DPPC phospholipid bilayers using temperature-controlled scanning force microscopy. Biophys. J . 86 (6), 3783–3793. https://doi.org/10.1529/biophysj.103.036681.
Li, M., Du, C., Guo, N., Teng, Y., Meng, X., Sun, H., Li, S., Yu, P., Galons, H., 2019. Composition design and medical application of liposomes. Eur. J. Med. Chem. 164, 640–653. https://doi.org/10.1016/j.ejmech.2019.01.007.
Liu, Y., Sun, J., Cao, W., Yang, J., Lian, H., Li, X., Sun, Y., Wang, Y., Wang, S., He, Z., 2011. Dual targeting folate-conjugated hyaluronic acid polymeric micelles for paclitaxel delivery. Int. J. Pharm. 421 (1), 160–169. https://doi.org/10.1016/j.ijpharm.2011.09.006.
Lombardo, D., Kiselev, M.A., 2022. Methods of liposomes preparation: formation and control factors of versatile nanocarriers for biomedical and nanomedicine application. Pharmaceutics 14 (3), 543. https://doi.org/10.3390/pharmaceutics14030543.
Machado, V., Morais, M., Medeiros, R., 2022. Hyaluronic acid-based nanomaterials applied to cancer: where are we now? Pharmaceutics 14 (10), 2092. https://doi.org/10.3390/pharmaceutics14102092.
Mahmoudi, R., Ashraf Mirahmadi-Babaheidri, S., Delaviz, H., Fouani, M.H., Alipour, M., Jafari Barmak, M., Christiansen, G., Bardania, H., 2021. RGD peptide-mediated liposomal curcumin targeted delivery to breast cancer cells. J. Biomater. Appl. 35 (7), 743–753. https://doi.org/10.1177/0885328220949367.
Mansoori, B., Mohammadi, A., Abedi-Gaballu, F., Abbaspour, S., Ghasabi, M., Yekta, R., Shirjang, S., Dehghan, G., Hamblin, M.R., Baradaran, B., 2020. Hyaluronic acid-decorated liposomal nanoparticles for targeted delivery of 5-fluorouracil into HT-29 colorectal cancer cells. J. Cell. Physiol. 235 (10), 6817–6830. https://doi.org/10.1002/jcp.29576.
Manzari-Tavakoli, A., Babajani, A., Tavakoli, M.M., Safaeinejad, F., Jafari, A., 2024. Integrating natural compounds and nanoparticle-based drug delivery systems: a novel strategy for enhanced efficacy and selectivity in cancer therapy. Cancer Med. 13 (5), e7010.
Mattiuzzi, C., Sanchis-Gomar, F., Lippi, G., 2019. Concise update on colorectal cancer epidemiology. Annals of Translational Medicine 7 (21), Article 21. https://doi.org/10.21037/atm.2019.07.91.
Mirone, G., Perna, S., Shukla, A., Marfe, G., 2016. Involvement of notch-1 in resistance to regorafenib in colon cancer cells. J. Cell. Physiol. 231 (5), 1097–1105. https://doi.org/10.1002/jcp.25206.
Misra, S., Hascall, V.C., Markwald, R.R., Ghatak, S., 2015. Interactions between hyaluronan and its receptors (CD44, RHAMM) regulate the activities of inflammation and cancer. Front. Immunol. 6, 201. https://doi.org/10.3389/fimmu.2015.00201.
Najafi, S., Rahimi, Z., Mansoori, B., Mohammadi, A., Mohammadnejad, F., Amini, M., Mokhtazadeh, A., Asadzadeh, Z., Chi-Shing Cho, W., Baradaran, B., 2023. CD44 suppression improved the chemosensitivity of HT-29 colorectal cancer cells to 5-fluorouracil and inhibited cell migration. Adv. Pharma. Bull. 13 (3), 551–562. https://doi.org/10.34172/apb.2023.053.
Olusanya, T.O.B., Haj Ahmad, R.R., Ibegbu, D.M., Smith, J.R., Elkordy, A.A., 2018. Liposomal drug delivery systems and anticancer drugs. Molecules : J. Synthetic Chem. Nat. Product Chem. 23 (4), 907. https://doi.org/10.3390/molecules23040907.
Pan, J., Heberle, F.A., Tristram-Nagle, S., Szymanski, M., Koepfinger, M., Katsaras, J., Kučerka, N., 2012. Molecular structures of fluid phase phosphatidylglycerol bilayers as determined by small angle neutron and X-ray scattering. BBA 1818 (9), 2135–2148. https://doi.org/10.1016/j.bbamem.2012.05.007.
Pandelidou, M., Dimas, K., Georgopoulos, A., Hatziantoniou, S., Demetzos, C., 2011. Preparation and characterization of lyophilised egg PC liposomes incorporating curcumin and evaluation of its activity against colorectal cancer cell lines. J. Nanosci. Nanotechnol. 11 (2), 1259–1266. https://doi.org/10.1166/jnn.2011.3093.
Pandolfi, L., Frangipane, V., Bocca, C., Marengo, A., Tarro Genta, E., Bozzini, S., Morosini, M., D'Amato, M., Vitulo, S., Monti, M., Comolli, G., Scupoli, M.T., Fattal, E., Arpicco, S., Meloni, F., 2019. Hyaluronic acid–decorated liposomes as innovative targeted delivery system for lung fibrotic cells. Molecules 24 (18), 3291. https://doi.org/10.3390/molecules24183291.
Plumb, J.A., 1999. Cell sensitivity assays: the MTT assay. Methods Mol. Med. 28, 25–30. https://doi.org/10.1385/1-59259-687-8:25.
Priyadarsini, K.I., 2014. The chemistry of curcumin: From extraction to therapeutic agent. Molecules (Basel, Switzerland) 19 (12), 20091–20112. https://doi.org/10.3390/molecules191220091.
Qhattal, H.S.S., Hye, T., Alali, A., Liu, X., 2014. Hyaluronan polymer length, grafting density, and surface poly(ethylene glycol) coating influence in vivo circulation and tumor targeting of hyaluronan-grafted liposomes. ACS Nano 8 (6), 5423–5440. https://doi.org/10.1021/nn405839n.
Raju, R., Abuwatfa, W.H., Pitt, W.G., Husseini, G.A., 2023. Liposomes for the treatment of brain cancer-a review. Pharmaceuticals (Basel, Switzerland) 16 (8), 1056. https://doi.org/10.3390/ph16081056.
Ravar, F., Saadat, E., Gholami, M., Dehghankelishadi, P., Mahdavi, M., Azami, S., Dorkoosh, F.A., 2016. Hyaluronic acid-coated liposomes for targeted delivery of paclitaxel, in-vitro characterization and in-vivo evaluation. J. Control. Release 229, 10–22. https://doi.org/10.1016/j.jconrel.2016.03.012.
Rippe, M., Cosenza, V., Auzély-Velty, R., 2019. Design of soft nanocarriers combining hyaluronic acid with another functional polymer for cancer therapy and other biomedical applications. Pharmaceutics 11 (7), 338. https://doi.org/10.3390/pharmaceutics11070338.
Ruozi, B., Belletti, D., Tombesi, A., Tosi, G., Bondioli, L., Forni, F., Vandelli, M.A., 2011. AFM, ESEM, TEM, and CLSM in liposomal characterization: a comparative study. Int. J. Nanomed. 6, 557–563. https://doi.org/10.2147/IJN.S14615.
Sang, R., Stratton, B., Engel, A., Deng, W., 2021. Liposome technologies towards colorectal cancer therapeutics. Acta Biomater. 127, 24–40. https://doi.org/10.1016/j.actbio.2021.03.055.
Scaria, B., Sood, S., Raad, C., Khanafer, J., Jayachandiran, R., Pupulin, A., Grewal, S., Okoko, M., Arora, M., Miles, L., Pandey, S., 2020. Natural Health Products (NHP's) and natural compounds as therapeutic agents for the treatment of cancer; mechanisms of anti-cancer activity of natural compounds and overall trends. Int. J. Mol. Sci. 21 (22), 8480. https://doi.org/10.3390/ijms21228480.
Sesarman, A., Tefas, L., Sylvester, B., Licarete, E., Rauca, V., Luput, L., Patras, L., Banciu, M., Porfire, A., 2018. Anti-angiogenic and anti-inflammatory effects of long-circulating liposomes co-encapsulating curcumin and doxorubicin on C26 murine colon cancer cells. Pharmacological Reports: PR 70 (2), 331–339. https://doi.org/10.1016/j.pharep.2017.10.004.
Sharifi-Rad, J., Rayess, Y.E., Rizk, A.A., Sadaka, C., Zgheib, R., Zam, W., Sestito, S., Rapposelli, S., Neffe-Skocińska, K., Zielińska, D., Salehi, B., Setzer, W.N., Dosoky, N. S., Taheri, Y., El Beyrouthy, M., Martorell, M., Ostrander, E.A., Suleria, H.A.R., Cho, W.C., Martins, N., 2020. Turmeric and its major compound curcumin on health: bioactive effects and safety profiles for food, pharmaceutical, biotechnological and medicinal applications. Front. Pharmacol. 11, 01021. https://doi.org/10.3389/fphar.2020.01021.
Strumberg, D., Schultheis, B., 2012. Regorafenib for cancer. Expert Opin. Invest. Drugs 21 (6), 879–889. https://doi.org/10.1517/13543784.2012.684752.
Surace, C., Arpicco, S., Dufaÿ-Wojcicki, A., Marsaud, V., Bouclier, C., Clay, D., Cattel, L., Renoir, J.-M., Fattal, E., 2009. Lipoplexes targeting the CD44 hyaluronic acid receptor for efficient transfection of breast cancer cells. Mol. Pharm. 6 (4), 1062–1073. https://doi.org/10.1021/mp800215d.

Szoka, F., Papahadjopoulos, D., 1980. Comparative properties and methods of preparation of lipid vesicles (liposomes). Annu. Rev. Biophys. Bioeng. 9, 467–508. https://doi.org/10.1146/annurev.bb.09.060180.002343.

Tefas, L.R., Sylvester, B., Tomuta, I., Sesarman, A., Licarete, E., Banciu, M., Porfire, A., 2017. Development of antiproliferative long-circulating liposomes co-encapsulating doxorubicin and curcumin, through the use of a quality-by-design approach. Drug Des. Devel. Ther. 11, 1605–1621. https://doi.org/10.2147/DDDT.S129008.

Tiantian, Y., Wenji, Z., Mingshuang, S., Rui, Y., Shuangshuang, S., Yuling, M., Jianhua, Y., Xinggang, Y., Shujun, W., Weisan, P., 2014. Study on intralymphatic-targeted hyaluronic acid-modified nanoliposome: Influence of formulation factors on the lymphatic targeting. Int. J. Pharm. 471 (1–2), 245–257. https://doi.org/10.1016/j.ijpharm.2014.05.027.

van Meerloo, J., Kaspers, G.J.L., Cloos, J., 2011. Cell sensitivity assays: the MTT assay. Methods Mol. Biol. (CliftonN.J.) 731, 237–245. https://doi.org/10.1007/978-1-61779-080-5_20.

Wang, S., Chen, Y., Guo, J., Huang, Q., 2023. Liposomes for tumor targeted therapy: a review. Int. J. Mol. Sci. 24 (3), 2643. https://doi.org/10.3390/ijms24032643.

Wang, J., Liu, D., Guan, S., Zhu, W., Fan, L., Zhang, Q., Cai, D., 2020. Hyaluronic acid-modified liposomal honokiol nanocarrier: enhance anti-metastasis and antitumor efficacy against breast cancer. Carbohydr. Polym. 235, 115981 https://doi.org/10.1016/j.carbpol.2020.115981.

Wilhelm, S.M., Dumas, J., Adnane, L., Lynch, M., Carter, C.A., Schütz, G., Thierauch, K.-H., Zopf, D., 2011. Regorafenib (BAY 73–4506): A new oral multikinase inhibitor of angiogenic, stromal and oncogenic receptor tyrosine kinases with potent preclinical antitumor activity. Int. J. Cancer 129 (1), 245–255. https://doi.org/10.1002/ijc.25864.

William, B., Noémie, P., Brigitte, E., Géraldine, P., 2020. Supercritical fluid methods: an alternative to conventional methods to prepare liposomes. Chem. Eng. J. 383, 123106 https://doi.org/10.1016/j.cej.2019.123106.

Wong, K.E., Ngai, S.C., Chan, K.-G., Lee, L.-H., Goh, B.-H., Chuah, L.-H., 2019. Curcumin nanoformulations for colorectal cancer: a review. Front. Pharmacol. 10. https://www.frontiersin.org/articles/10.3389/fphar.2019.00152.

Xie, Y.-H., Chen, Y.-X., Fang, J.-Y., 2020. Comprehensive review of targeted therapy for colorectal cancer. Signal Transduct. Target. Ther. 5 (1) https://doi.org/10.1038/s41392-020-0116-z. Article 1.

Xu, Y., Yao, Y., Wang, L., Chen, H., Tan, N., 2021. Hyaluronic acid coated liposomes co-delivery of natural cyclic peptide RA-XII and mitochondrial targeted photosensitizer for highly selective precise combined treatment of colon cancer. Int. J. Nanomed. 16, 4929–4942. https://doi.org/10.2147/IJN.S311577.

Yang, X.-Y., Li, Y.-X., Li, M., Zhang, L., Feng, L.-X., Zhang, N., 2013. Hyaluronic acid-coated nanostructured lipid carriers for targeting paclitaxel to cancer. Cancer Lett. 334 (2), 338–345. https://doi.org/10.1016/j.canlet.2012.07.002.

Ye, P., Zhang, W., Yang, T., Lu, Y., Lu, M., Gai, Y., Ma, X., Xiang, G., 2014. Folate receptor-targeted liposomes enhanced the antitumor potency of imatinib through the combination of active targeting and molecular targeting. Int. J. Nanomed. 9 (1), 2167–2178. https://doi.org/10.2147/IJN.S60178.

Zhang, H., 2017. Thin-Film Hydration Followed by Extrusion Method for Liposome Preparation. Methods Mol. Biol. (CliftonN.J.) 1522, 17–22. https://doi.org/10.1007/978-1-4939-6591-5_2.

Zhao, Y., Zhang, T., Duan, S., Davies, N.M., Forrest, M.L., 2014. CD44-Tropic polymeric nanocarrier for breast cancer targeted rapamycin chemotherapy. Nanomed. Nanotechnol. Biol. Med. 10 (6), 1221–1230. https://doi.org/10.1016/j.nano.2014.02.015.

Zhu, T.F., Budin, I., Szostak, J.W., 2013. Vesicle extrusion through polycarbonate track-etched membranes using a hand-held mini-extruder. Methods Enzymol. 533, 275–282. https://doi.org/10.1016/B978-0-12-420067-8.00021-0.